ACS Catalysis

Research Article

pubs.acs.org/acscatalysis

Single-Site Palladium(II) Catalyst for Oxidative Heck Reaction: Catalytic Performance and Kinetic Investigations

Hui Duan,[†] Menghuan Li,[†] Guanghui Zhang,[‡,§] James R. Gallagher,[§] Zhiliang Huang,[‡,§] Yu Sun,[‡] Zhong Luo,[†] Hongzhong Chen,[†] Jeffrey T. Miller,[§] Ruqiang Zou,[∥] Aiwen Lei,*[,‡] and Yanli Zhao*[,†,⊥]

[†]Division of Chemistry and Biological Chemistry, School of Physical & Mathematical Sciences, Nanyang Technological University, 21 Nanyang Link, 637371 Singapore

[‡]College of Chemistry and Molecular Sciences, Wuhan University, Wuhan, Hubei 430072, People's Republic of China

[§]Chemical Sciences and Engineering Division, Argonne National Laboratory, Argonne, Illinois 60439, United States

[∥] Department of Materials Science and Engineering, College of Engineering, Peking University, Beijing 100871, People's Republic of China

[⊥]School of Materials Science and Engineering, Nanyang Technological University, 639798 Singapore

Supporting Information

ABSTRACT: The development of organometallic single-site catalysts (SSCs) has inspired the designs of new heterogeneous catalysts with high efficiency. Nevertheless, the application of SSCs in certain modern organic reactions, such as C−C bond formation reactions, has still been less investigated. In this study, a single-site Pd(II) catalyst was developed, where 2,2′-bipyridine-grafted periodic mesoporous organosilica (PMO) was employed as the support of a Pd(II) complex. The overall performance of the single-site Pd(II) catalyst in the oxidative Heck reaction was then investigated. The investigation results show that the catalyst displays over 99% selectivity for the product formation with high reaction yield. Kinetic profiles further confirm its high catalytic efficiency, showing that the rate constant is nearly 40 times higher than that for the free Pd(II) salt. X-ray absorption spectroscopy reveals that the catalyst has remarkable lifetime and recyclability.

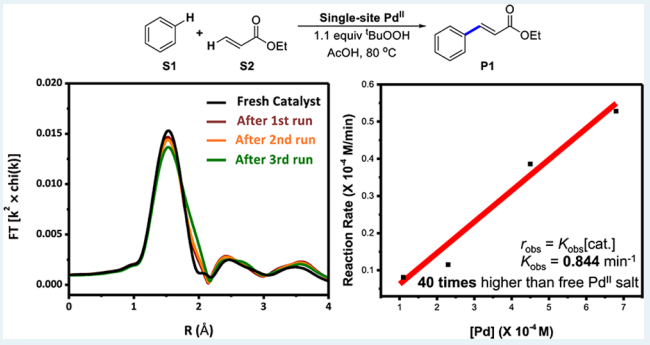

KEYWORDS: *C−H olefination, cross-coupling reactions, oxidative Heck reaction, periodic mesoporous organosilica, single-site Pd(II) catalyst*

1. INTRODUCTION

Due to its high atom economy and low cost of reactants, palladium-catalyzed C−C bond formation based on C−H functionalization has become an important topic in modern organic chemistry.[1−5] Studies in this field have been focused on developing highly regioselective reactions or enhancing the catalytic activity by using particular ligands in homogeneous catalytic systems.[6−9] However, there is still a general lack of palladium-catalyzed processes that can retain high reactivity and high recovery rate of the catalyst at the same time, both of which are of great importance in catalysis. Since the primary valence-state change of palladium during the C−C bond formation reactions is between Pd(0) and Pd(II),[10,11] the formation of palladium aggregates is common in most palladium-based homogeneous catalytic processes, which significantly reduces the catalytic activity. For many catalysts, it is already known that desirable catalytic properties are associated with well-defined active sites containing just a few or even a single metal atom.[12−20] Thus, it is important to develop efficient single-site palladium catalysts and investigate their catalytic performance.

Since the earliest application of catalytic cracking processes in the petrochemical industry, the utilization of porous materials in catalysis has been extensively studied and widely applied.[21−25] Numerous mesoporous materials have been synthesized. Owing to their unique nanostructures, those mesoporous materials provide ideal supports for single-site metal catalysts.[26−32] Palladium-containing mesoporous materials have been investigated as heterogeneous catalysts for coupling reactions.[25,33−42] However, the applications of those catalysts were limited in traditional coupling reactions (between C−M and C−X) with palladium nanoparticles or leached homogeneous Pd(0) as the main active species.[25,43−46] Since mechanistic studies revealed that many C−H functionalization reactions start from Pd(II),[47−49] the application of palladium-

Received: March 17, 2015
Revised: May 11, 2015
Published: May 12, 2015

DOI: 10.1021/acscatal.5b00569
ACS Catal. 2015, 5, 3752−3759

nanoparticle-containing mesoporous materials in these reactions was undesirable. In order to avoid the drawbacks of palladium nanoparticles and expand the application scope of palladium-containing mesoporous catalysts, we sought to determine if a single-site Pd(II) C−H/olefin coupling catalyst could be developed (Scheme 1), which should possess higher

Scheme 1. Palladium-Catalyzed C−H Olefination Reactions in Previous Work and in This Work

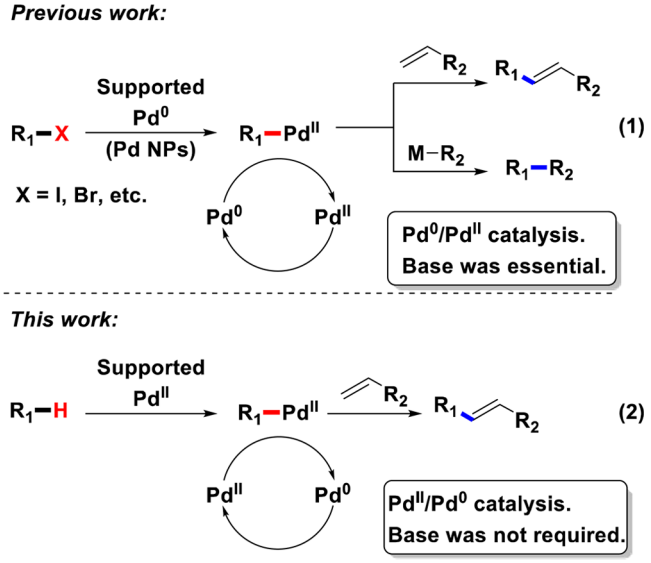

atom economy and lower production cost for substrates. Furthermore, without the presence of base, the integrity of the mesoporous framework would likely be maintained. It is highly possible that this design would prolong the lifetime of the catalyst.

Recently, oxidative coupling reactions have attracted much attention.[49−53] These reactions provide new approaches for carbon−carbon and carbon−heteroatom bond formations. The oxidative Heck reaction is one of these reactions, which has been widely investigated.[3,47,54−56] Up to now, most of the explorations of the Fujiwara−Moritani reaction have focused on the regioselectivity of arenes. Yu and co-workers made a breakthrough by avoiding the use of excess simple arenes in the substrates.[57] Previous work demonstrated a plausible mechanism where the activation of a C−H bond can only be initiated by Pd(II) in the reaction, while the agglomeration of Pd(0) was the main reason for the deactivation of the catalyst (Scheme 2).[47,58] Thus, the pursuit of prolonging the catalyst lifetime in the oxidative Heck reaction is of great importance. The introduction of a single-site catalyst may provide an ideal approach to improve the lifetime and catalytic efficiency. Herein, we communicate our recent results on the catalytic performance of single-site Pd-containing periodic mesoporous organosilica (PMO) in the oxidative Heck reaction.

2. RESULTS AND DISCUSSION

Initially, we started the research by investigating the oxidative Heck reactions that were catalyzed by Pd(II) metal complex grafted PMO. As pyridine-based ligands have shown potency in the C−H olefination reactions,[8,47,49,56,59−61] a bipyridine-containing organosilica precursor (ligand **1**) was designed and synthesized (see Scheme S1 in the Supporting Information for more details). The 2,2′-bipyridine-functionalized MCM type

Scheme 2. Palladium-Catalyzed C−H Olefination Reactions and Deactivation of the Catalyst

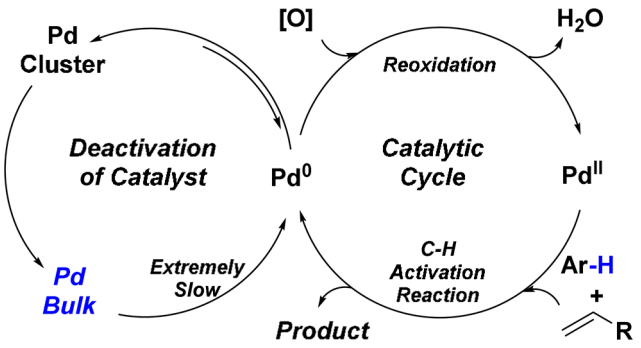

PMO was prepared using a procedure adapted from the literature.[62−67] Palladium acetate was subsequently loaded into 2,2′-bipyridine-grafted PMO to form the Pd(II) complex in the PMO (Scheme 3).

Scheme 3. Preparation of Pd^{II} Complex Functionalized MCM-41 Type PMO

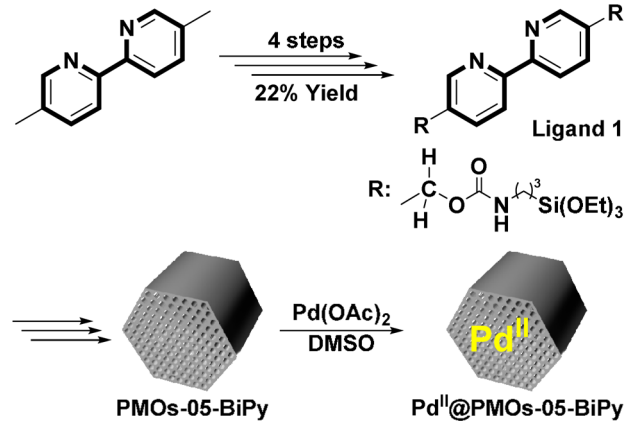

A series of PMOs were prepared containing ligand **1** and tetraethyl orthosilicate (TEOS) in mole fractions of 0.10:0.90 (PMOs-10-BiPy), 0.05:0.95 (PMOs-05-BiPy), and 0.00:1.00 (PMOs) calculated on the basis of the Si contributions. Surface passivation was achieved by conjugating Et_3SiOEt onto PMOs-05-BiPy to prepare the surface-passivated PMOs (Si-PMOs-05-BiPy). As no orderly mesoporous structure was found in the case of PMOs-10-BiPy, we primarily focused on investigating the properties and performance of PMOs-05-BiPy. To verify the structures of PMOs-05-BiPy and corresponding palladium-loaded Pd^{II}@PMOs-05-BiPy catalyst, the samples were characterized using transmission electron microscopy (TEM), powder X-ray diffraction (XRD), N_2 adsorption/desorption measurement, FT-IR, and thermogravimetric analysis (TGA) techniques. The TEM images (Figure S2 in the Supporting Information) and powder XRD results (Figure S3 in the Supporting Information) confirmed that the sample PMOs-05-BiPy was of MCM-41 type. The BET surface area, pore size, and pore volume were derived from the N_2 adsorption/desorption isotherm (Figures S4 and S5a in the Supporting Information). The FT-IR (Figure S5b in the Supporting Information) and contact angle measurements (Figure S6 and Table S1 in the Supporting Information) were employed to verify the passivation efficiency of Si-PMOs-05-BiPy. FT-IR

DOI: 10.1021/acscatal.5b00569
ACS Catal. 2015, 5, 3752−3759

(Figure S7 and Table S2 in the Supporting Information) and TGA (Figure S8 in the Supporting Information) data confirmed that the ligand was immobilized into PMOs-05-BiPy.

Previous reports[33,35,41] on Pd-containing PMO catalysts indicated that the Pd nanoparticles were unavoidable. Thus, it is necessary to study and improve the Pd(II) loading process, since the Pd nanoparticles cannot catalyze the C−H olefination reactions. According to the literature reports, dimethyl sulfoxide (DMSO) is capable of stabilizing the Pd(II) salt.[68−70] On the basis of this rationale, several methods of loading palladium into PMO were evaluated. As shown in Figure 1, no Pd nanoparticles were found when loading the Pd^{II} salt in DMSO at room temperature (Figure 1b, Pd^{II}@PMOs-05-BiPy prepared from method A in the Supporting Information). In order to further increase the Pd^{II} concentration in PMO, we kept DMSO as the loading solvent while changing other conditions, such as raising the loading temperature to 80 °C and prolonging the loading time to overnight (Figure 1c from method B). However, Pd nanoparticles appeared in the resulting PMO in these cases. Thus, Pd^{II}@PMOs-05-BiPy prepared from method A was eventually chosen for the subsequent experiments. Pd nanoparticles could evidently be observed in the TEM image (Figure 1d) when EtOH was employed as the loading solvent (method C), which is consistent with previous reports.

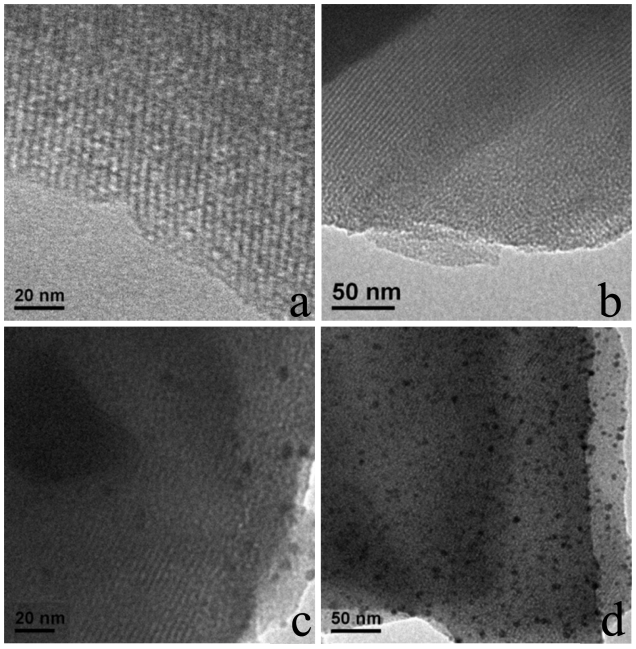

Figure 1. (a) TEM image of PMOs-05-BiPy. (b) TEM image of Pd^{II}@PMOs-05-BiPy prepared from method A. (c) TEM image of the catalyst prepared from method B. (d) TEM image of the catalyst prepared from method C.

After Pd^{II}@PMOs-05-BiPy was obtained using method A, its palladium content (1.1×10^{-4} mmol/mg, 1.2 wt %) was measured by inductively coupled plasma mass spectrometry (ICPMS). The molar ratio (4.1:1.0) between 2,2′-bipyridine and $Pd(OAc)_2$ was obtained after analyzing the palladium content with the TGA data (Figure S8 in the Supporting Information). Due to the mesoporous feature of the materials and low palladium content, no palladium signal could be observed by either X-ray photoelectron spectroscopy (XPS) and energy-dispersive X-ray spectroscopy (EDS). As shown in Figure 2, in comparison to palladium foil Pd(0) or/and $Pd(OAc)_2$, the Pd K-edge XANES spectrum of fresh Pd^{II}@PMOs-05-BiPy catalyst was very similar to that of PdO and $Pd(OAc)_2$, giving an edge energy of 24353.8 eV. The observation confirms the existence of Pd(II) species in PMOs.[71−73]

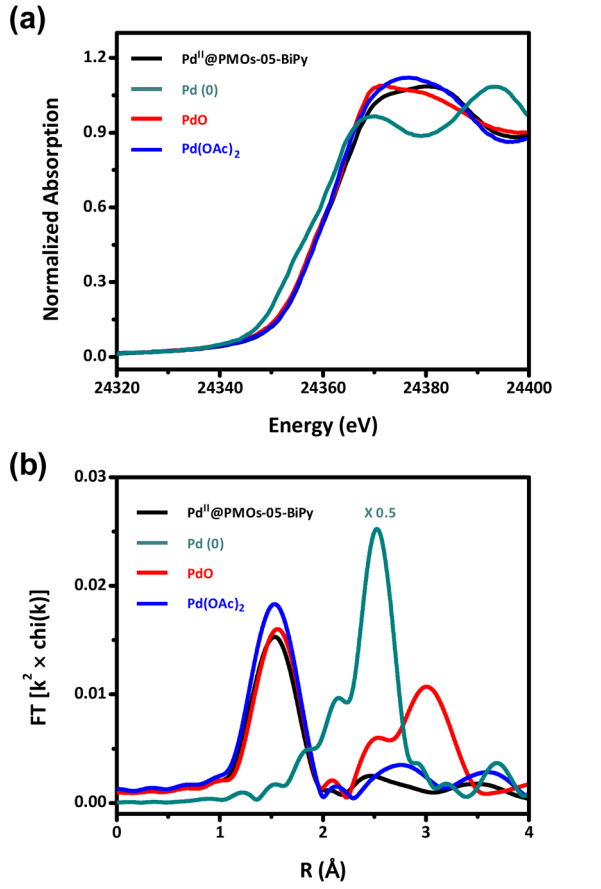

Figure 2. (a) XANES spectra of fresh Pd^{II}@PMOs-05-BiPy catalyst and reference materials. (b) k^2-weighted Fourier transform magnitudes of fresh Pd^{II}@PMOs-05-BiPy catalyst and reference materials. Fourier transform ranges are as follows: fresh catalyst, 3.08−12.72 $Å^{-1}$; Pd(0), 2.25−14.59 $Å^{-1}$; PdO, 3.10−11.57 $Å^{-1}$; $Pd(OAc)_2$. 3.05−12.02 $Å^{-1}$.

In order to maintain the Pd^{II} species after the catalytic process for reuse, the reaction conditions of the oxidative Heck reaction with the Pd^{II}@PMOs-05-BiPy catalyst were optimized using a model reaction between benzene and ethyl acrylate. As shown in Table S3 in the Supporting Information, an acceptable yield was obtained when ^{t}BuOOH was employed as the reoxidation reagent. We have also tried some other oxidants, such as oxone, potassium persulfate, and (diacetoxyiodo)benzene. On consideration of the product selectivity and catalyst recovery, ^{t}BuOOH was the best reagent for this C−H olefination reaction. More importantly, no Pd nanoparticles were observed from the recycled catalyst, which proved that the present design concept is reasonable and workable. Furthermore, from the control experiments shown in Table S3, it could be concluded that the presence of a 2,2′-bipyridine unit in the framework is capable of constraining the palladium atom through coordination, and the mesoporous framework could prevent the agglomeration of Pd(0) during

DOI: 10.1021/acscatal.5b00569
ACS Catal. 2015, 5, 3752−3759

the catalytic cycles. Both the 2,2′-bipyridine unit and the mesoporous framework were essentially required in the C−H/olefin coupling reaction catalyzed by this PMO-supported Pd(II).

It is well-known that the external and internal surfaces of PMOs are covered by silanol groups. Together with the specific nanostructure, silanols inside the channels may influence the diffusion of the reaction substrates significantly. The experimental results in Figure S9 in the Supporting Information show that an appropriate concentration ratio of benzene to ethyl acrylate in the model reaction was essential to facilitate the C−H activation and catalytic cycle for the best yield.

Table 1 shows the results of the model reaction catalyzed by different catalysts under the optimal condition from Table S3 and Figure S9 in the Supporting Information. In the model reaction, Pd^{II}@PMOs-05-BiPy prepared from method A (Table 1, entry 1) afforded a yield of 58%. When the catalyst prepared through method B ([Pd] = 2.9×10^{-4} mmol/mg, 3.2 wt %) was employed, the resulting yield dropped to 42% (Table 1, entry 2). This difference may be caused by lower Pd(II) content from method B. When palladium on PMOs-05-BiPy was mostly in the form of Pd nanoparticles (prepared from method C, [Pd] = 4.1×10^{-4} mmol/mg, 4.5 wt %), the model reaction showed 11% yield (Table 1, entry 3). Without the 2,2′-bipyridine unit, silanol groups in PMOs alone did not have the ability to hold the palladium as Pd(II). Pd nanoparticles appeared when we tried to load Pd(II) into PMOs, and no activity was found in this model reaction (Table 1, entry 4). From entry 1 to entry 4, it could be concluded that the Pd nanoparticle formation is deleterious to the catalytic performance under the standard conditions. When the porous material was capped by a G4 dendrimer (dendrimer-Pd-PMO), only a small amount of product was observed by gas chromatography (Table 1, entry 5). The introduction of a bulky dendrimer unit to the PMO catalyst induces an obvious yield decrease, which may be on account of the restricted diffusion process of the reactants (more likely) or reduced palladium leaching to solution if the activity from the leached metal plays a role (less likely, but future work will explore this possibility). The selectivity was lower when using $Pd(OAc)_2$ as the catalyst (3,3-diphenylacrylic acid ethyl ester as the main byproduct; Table 1, entries 6 and 7).

The turnover numbers (TON) of different catalysts are also shown in Table 1. The TON of Pd^{II}@PMOs-05-Bipy was significantly higher than that of $Pd(OAc)_2$ (Table 1, entries 1, 6, and 7). A lower TON value (Table 2, entry 6) was obtained when 1.9 mmol % of $Pd(OAc)_2$ was employed as the catalyst. When the loading of $Pd(OAc)_2$ was decreased to 0.9 mmol % (Table 1, entry 7), the TON increased to 56. As expected, the TON increased to 128 when Pd^{II}@PMOs-05-Bipy was employed at a comparable palladium loading concentration (0.4 mmol %). Thus, the much higher reaction yield from Pd^{II}@PMOs-05-BiPy indicates that the reaction happens inside the porous framework. Even though the presence of Pd nanoparticles enhances the Pd concentration in the catalyst (Table 1, entry 2), the TON obtained (36) was unsatisfactory, as most of the palladium loaded in this method was Pd(0). In addition, an extremely low TON was observed from entry 3, which is similar to the situation in entry 2. These observations indicate that Pd nanoparticles have no catalytic activity in the C−H olefination reaction. Thus, the catalytic phenomenon could be attributed to the stabilization of active Pd(II) catalyst by the grafted 2,2′-bipyridine ligand on PMOs, retaining its catalytic activity.

After identifying the catalytic activity and optimized reaction conditions, we began our investigation into the scope of the reaction. As shown in Table 2, various arenes and olefins

Table 1. Effect of Different Catalysts for the Model Reaction[a]

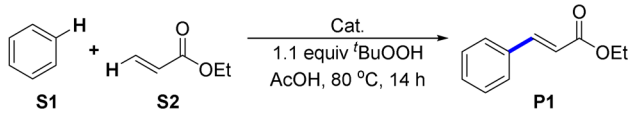

S1 S2 P1

entry	cat.	TON	selectivity (%)	yield (%)
1	Pd^{II}@PMOs-05-BiPy[b]	128	98	58
2	Pd′@PMOs-05-BiPy[c]	36	98	42
3	Pd″@PMOs-05-BiPy[d]	13	99	11
4	Pd″@PMOs[e]			trace
5	dendrimer-Pd-PMOs[f]			<5
6	$Pd(OAc)_2$ (2.0 mg)	37	88	66
7	$Pd(OAc)_2$ (0.5 mg)	56	92	24

[a]Reaction conditions: **S1** (20 mmol), **S2** (0.5 mmol), AcOH as the solvent (3.0 mL), 80 °C, 14 h. The conversion and selectivity were determined by GC with dodecane as the internal standard. [b]Catalyst was prepared through method A in the Supporting Information. A 20 mg portion of catalyst was used. [c]Catalyst was prepared through method B in the Supporting Information. A 20 mg portion of catalyst was used. [d]Catalyst was prepared through method C in the Supporting Information. A 20 mg portion of catalyst was used. [e]Catalyst without the 2,2′-bipyridine unit was prepared through method A in the Supporting Information. A 20 mg portion of catalyst was used. [f]The palladium content of this catalyst was 0.5 wt %.

Table 2. Substrate Scope of Single-Site Pd(II)-Catalyzed Oxidative Coupling of Arenes with Olefins[a]

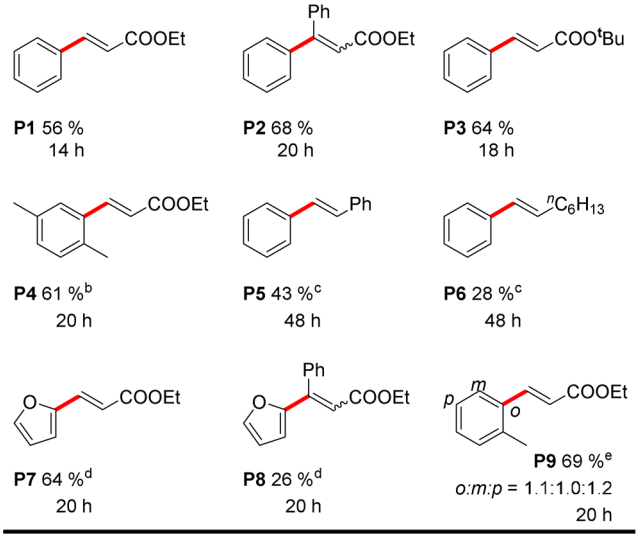

[a]Reaction conditions: 20 mg of Pd^{II}@PMOs-05-BiPy (0.4 mmol %) was used without indication, arene (20 mmol without indication), olefin (0.5 mmol), AcOH as the solvent (3.0 mL), 80 °C. [b]The molar ratio of arene and olefin was 60:1. [c]The molar ratio of arene and olefin was 60:1, and Pd′′@Si-PMOs-05-BiPy was used as the catalyst. [d]The molar ratio of furan and olefin was 20:1. [e]The molar ratio of arene and olefin was 60:1, and a mixture of *o*-, *m*-, and *p*-substituted products was obtained after workup (see Figure S10 in the Supporting Information for more details).

DOI: 10.1021/acscatal.5b00569
ACS Catal. 2015, 5, 3752−3759

underwent the oxidative olefination using the single-site Pd^{II}/^{t}BuOOH system. Although the catalyst loading was as low as 0.4 mmol %, acceptable yields were still obtained. The reactions of active olefins such as ethyl cinnamate and *tert*-butyl acrylate with benzene gave good yields of products **P2** and **P3**. When styrene and octene were used as the olefins to couple with benzene, the catalyst Pd′′@Si-PNOs-05-BiPy was needed to afford the products **P5** and **P6**, since the silanol groups on the catalyst had a noticeable effect on the diffusion process. The reaction between furan and compound **S2** also gave an isolated yield of 64% for the product **P7**. No regioselectivity was found when toluene was used as the arene substrate in the coupling reaction.

To expand the application scope of the catalyst, the model reaction was further optimized in a plug flow reactor (PFR, Scheme 4). The catalyst was packed into an empty HPLC

Scheme 4. Setup of the Plug Flow Reactor (PFR)

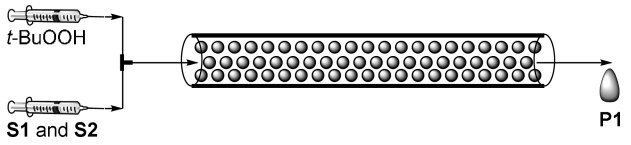

column (inside diameter 1 mm, length 100 mm). The two substrates and oxidant were separately filled into two syringes and then injected through the PFR by a syringe pump at a flow rate of 2 μL/min. The liquid hourly space velocity (LHSV) was 1.69 h^{-1}. The reaction yield was 12% with a selectivity of greater than 99%. The results indicate that the catalyst has an application potential in continuous-flow processes.

The recoverability of the catalysts is shown in Table 3. It can be observed that the catalytic effectiveness of Pd immobilized in

Table 3. Catalytic Performance of Recovered Pd^{II}@PMOs-05-BiPy in the Model Reaction[a]

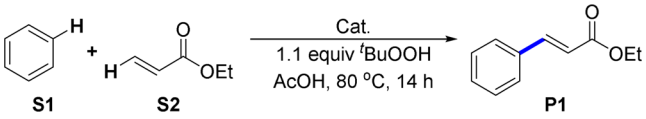

entry	Pd@PMOs-05-BiPy[b]	Pd:Bipy[c]	selectivity (%)	yield (%)	TON
1	first cycle	1.0:4.1	98	56	115
2	second cycle	1.0:4.5	99	48	110
3	third cycle	1.0:4.7	99	42	98
4	fourth cycle	1.0:5.1	99	39	97

[a]Reaction conditions: **S1** (20 mmol), **S2** (0.5 mmol), AcOH as the solvent (3.0 mL), 80 °C, 14 h, Pd^{II}@PMOs-05-BiPy (20 mg). The conversions were determined by GC with dodecane as the internal standard. [b]Fresh Pd^{II}@PMOs-05-BiPy was used in the first cycle, and then the catalyst was directly used in the following cycles after being recovered. [c]Molar ratios of palladium and ligand in PMOs.

the mesoporous materials (Pd^{II}@PMOs-05-Bipy) was still maintained in the fourth cycle. The excellent selectivity was obtained from all of the first four cycles with slightly decreasing yields in each successive test. The TON of catalyst Pd^{II}@PMOs-05-BiPy was also calculated. In comparison to previous TON records in the Pd-catalyzed oxidative Heck reaction,[74] this work reached a higher TON (420, from the first four runs) without the 1,4-benzoquinone participation. This result shows that the modified PMOs could be an excellent support for the single-site Pd(II) catalyst.

To investigate the oxidative states of the fresh catalyst and recycled Pd^{II}@PMOs-05-Bipy catalysts, X-ray absorption spectroscopy was carried out. As shown in Figure 3, the Pd K-edge XANES spectrum of the fresh catalyst shows an edge energy of 24353.8 eV, confirming the existence of Pd(II) species in Pd^{II}@PMOs-05-BiPy. In order to further explore the stability and recoverability of the developed catalyst, the XANES data for the recycled catalysts were collected as well. As shown in Figure 3a, the edge energies of the first recycled catalyst, the second recycled catalyst, and the third recycled catalyst were almost the same as that of the fresh catalyst. The EXAFS spectra were also recorded for the fresh and recovered catalysts (Figures S11−S14 and Tables S4 and S5 in the Supporting Information). The k_2-weighted *R*-space spectra are shown in Figure 3b. For the fresh catalyst, only a Pd(II) species was observed, which showed four-coordination at a distance of 2.03 Å. After the catalyst was reused three times, only a Pd(II) species was observed again, and the coordination number was the same as that of the fresh catalyst. The observations from both XANES and EXAFS spectra were further supported by TEM, where no Pd nanoparticles were found (Figure 3c,d). To the best of our knowledge, no catalytic activity of palladium black was found in the oxidative Heck reaction. Moreover, the controlled trials in Table 1 clearly show that the Pd nanoparticles cannot catalyze the oxidative Heck reaction.

On the basis of these comparison studies, it could be concluded that the mesoporous structure prevented Pd species from agglomeration and maintained it as Pd(II). It is expected that the metal sites in PMOs are isolated by the long channel structure and can retain their high activity during the catalytic process. Thus, the kinetic behavior of free $Pd(OAc)_2$ and the Pd^{II}@PMOs-05-BiPy catalyst was determined in the model reaction. As shown in Figures S15 and S16 in the Supporting Information, the kinetic plot of Pd^{II}@PMOs-05-BiPy shows a linear increase of conversion with time, which is similar to that for free $Pd(OAc)_2$. This observation suggests that the reaction rate is independent of concentrations [**S2**] and [^{t}BuOOH], showing zero-order kinetic behavior in [**S2**] and [^{t}BuOOH].

After more kinetic data were collected, a positive linear dependence on the [Pd] concentration was discovered, which revealed the first-order kinetic behavior in [Pd]. The linear relationship between the rate constants and [Pd] is shown in Figure 4. Although the mesoporous structure might theoretically impede the mass transfer process, the rate constant of Pd^{II}@PMOs-05-BiPy was as high as 0.844 min^{-1}. In compared to the rate constant (0.022 min^{-1}) of free $Pd(OAc)_2$ shown in Figure S15 in the Supporting Information, this result indicates that the catalytic efficiency of the Pd species in Pd^{II}@PMOs-05-BiPy was much higher than that of free $Pd(OAc)_2$ in the model reaction. Thus, the ligand-grafted mesoporous materials are a promising scaffold for single-site Pd(II) catalysts.

The kinetic profiles indicate that reoxidation and olefin insertion were not involved in rate-determining steps under the conditions. To gather more information about the effect of porous materials in this reaction, the kinetic isotope experiments (KIE) were performed to further investigate the catalytic mechanism (Figure 4 and Table S6 in the Supporting Information). By using Pd^{II}@PMOs-05-BiPy, the measured K_H/K_D value was 3.6, indicating that the C−H bond cleavage is still involved in the rate-limiting step. A proposal for the catalytic cycle is described in Scheme 5. After the C−H cleavage on Pd(II), the olefin would be coordinated to the Pd(II) intermediate generated in said process. Followed by

DOI: 10.1021/acscatal.5b00569
ACS Catal. 2015, 5, 3752−3759

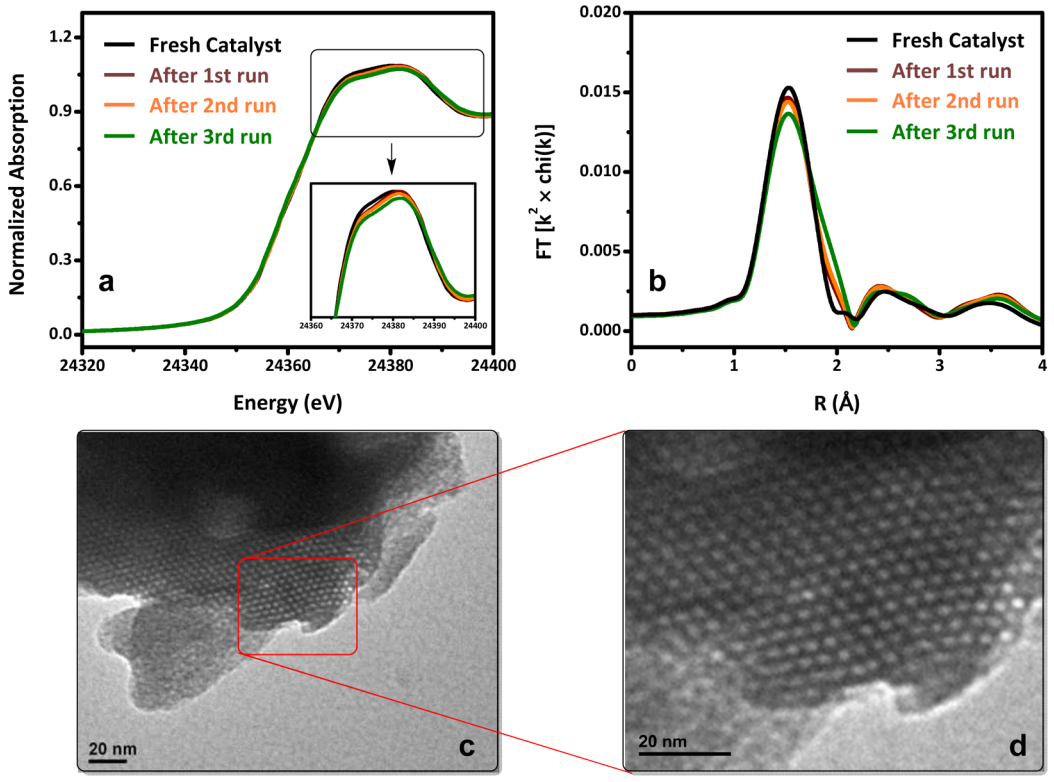

Figure 3. (a) XANES spectra of the fresh and recycled Pd^{II}@PMOs-05-Bipy catalysts. (b) k^2-weighted Fourier transform magnitudes of the fresh and used Pd(II) catalysts. Fourier transform ranges are given as follows: fresh catalyst, 3.08−12.72 $Å^{-1}$; recycled catalyst after first run, 3.09−12.81 $Å^{-1}$; recycled catalyst after second run, 3.08−12.96 $Å^{-1}$; recycled catalyst after third run, 3.10−13.061 $Å^{-1}$. (c, d) TEM images of the recycled catalyst after the third run.

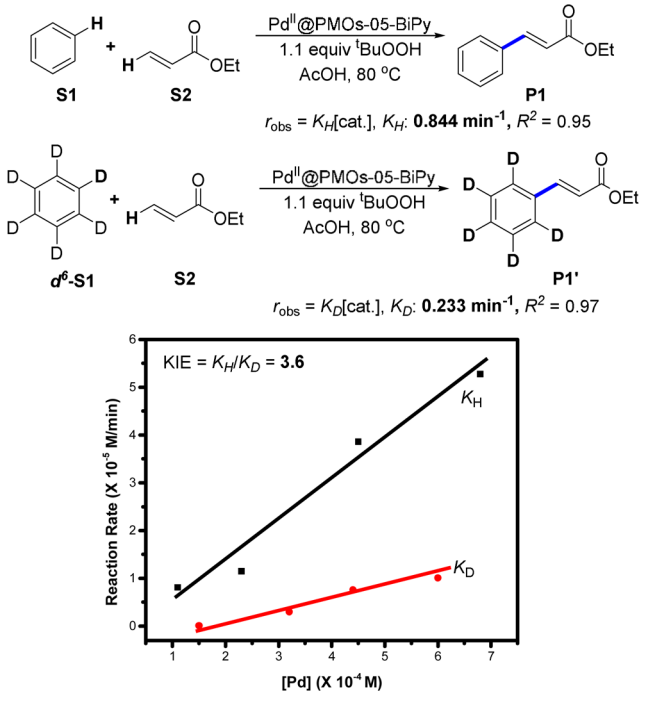

Figure 4. Kinetic profile of single-site Pd(II)-catalyzed oxidative Heck reaction. K_H is the rate constant from the reaction of benzene (**S1**), and K_D is the rate constant from the reaction of d_6-benzene (d_6-**S1**).

olefin insertion and β-H elimination, the new C−C bond was formed, thus giving the desired product together with Pd(0) species after reductive elimination, the latter of which can be reoxidized to Pd(II) and readily join the next catalytic cycle. PMOs-05-BiPy could prevent the agglomeration of Pd(0) and prolong the catalyst lifetime.

Scheme 5. Proposed Catalytic Cycle

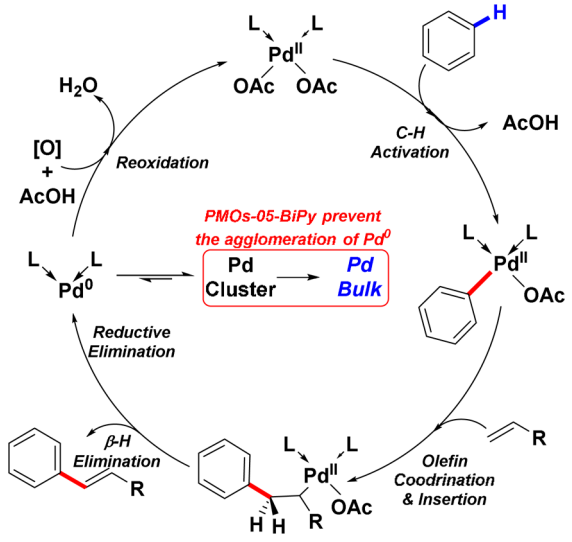

3. CONCLUSIONS

In summary, for the first time we have investigated the feasibility of using 2,2′-bipyridine-grafted periodic mesoporous organosilica (PMO) as a support of single-site Pd(II) catalyst for catalyzing C−H olefination reactions. The immobilized Pd(II) in PMO has shown catalytic activity higher than that of

DOI: 10.1021/acscatal.5b00569
ACS Catal. 2015, 5, 3752−3759

the corresponding homogeneous $Pd(OAc)_2$, which has been verified by kinetic profiles and kinetic isotope experiments. Its catalytic activity is also effective in the plug flow reactor. Furthermore, several different arenes and olefins have been tested as substrates and acceptable yields have been obtained under low Pd(II) loading. The XANES/EXAFS spectra have demonstrated that the Pd(II) species was the active catalyst in the reaction. In addition, the developed catalyst could be readily recycled with little loss in activity. Thus, this work presents a strategy of integrating active single-site catalysts with the PMO platform for specific organic reactions, offering a new generation of catalysts for the pharmaceutical industry.

■ ASSOCIATED CONTENT

Supporting Information

The Supporting Information is available free of charge on the ACS Publications website at DOI: 10.1021/acscatal.5b00569.

Experimental procedures and characterization data for all materials and compounds, TEM and HRTEM images, powder XRD, TGA, N_2 adsorption/desorption isotherms, FT-IR spectra, X-ray absorption spectra, kinetic data, and ^1H and ^{13}C NMR spectra of the products (PDF)

■ AUTHOR INFORMATION

Corresponding Authors

*E-mail for A.L.: aiwenlei@whu.edu.cn.
*E-mail for Y.Z.: zhaoyanli@ntu.edu.sg.

Notes

The authors declare no competing financial interest.

■ ACKNOWLEDGMENTS

This research was supported by the National Research Foundation (NRF), Prime Minister's Office, Singapore, under its NRF Fellowship (NRF2009NRF-RF001-015), and Campus for Research Excellence and Technological Enterprise (CREATE) Programme—Singapore Peking University Research Centre for a Sustainable Low-Carbon Future, as well as the NTU-A*Star Silicon Technologies Centre of Excellence under grant No. 112 351 0003. The use of the Advanced Photon Source was supported by the U.S. Department of Energy, Office of Science, and Office of Basic Energy Sciences under contract No. DE-AC02-06CH11357. MRCAT operations were supported by the U.S. Department of Energy and the MRCAT member institutions.

■ REFERENCES

(1) Daugulis, O.; Do, H.-Q.; Shabashov, D. *Acc. Chem. Res.* **2009**, *42*, 1074−1086.
(2) Hashiguchi, B. G.; Bischof, S. M.; Konnick, M. M.; Periana, R. A. *Acc. Chem. Res.* **2012**, *45*, 885−898.
(3) Sigman, M. S.; Werner, E. W. *Acc. Chem. Res.* **2012**, *45*, 874−884.
(4) Li, B.; Dixneuf, P. H. *Chem. Soc. Rev.* **2013**, *42*, 5744−5767.
(5) Mousseau, J. J.; Charette, A. B. *Acc. Chem. Res.* **2013**, *46*, 412−424.
(6) Fairlamb, I. J. S. *Chem. Soc. Rev.* **2007**, *36*, 1036−1045.
(7) Seregin, I. V.; Gevorgyan, V. *Chem. Soc. Rev.* **2007**, *36*, 1173−1193.
(8) Lyons, T. W.; Sanford, M. S. *Chem. Rev.* **2010**, *110*, 1147−1169.
(9) Neufeldt, S. R.; Sanford, M. S. *Acc. Chem. Res.* **2012**, *45*, 936−946.
(10) Johansson, S. C. C. C.; Kitching, M. O.; Colacot, T. J.; Snieckus, V. *Angew. Chem., Int. Ed.* **2012**, *51*, 5062−5085.
(11) Amatore, C.; Jutand, A. In *Handbook of Organopalladium Chemistry for Organic Synthesis*; Wiley: New York, 2002; Vol. *1*, pp 943−972.
(12) Grasselli, R. K. *Top. Catal.* **2001**, *15*, 93−101.
(13) Millet, J.-M. M.; Vedrine, J. C. *Top. Catal.* **2001**, *15*, 139−144.
(14) Thomas, J. M. *Top. Catal.* **2001**, *15*, 85−91.
(15) Volta, J.-C. *Top. Catal.* **2001**, *15*, 121−129.
(16) Yang, X.-F.; Wang, A.; Qiao, B.; Li, J.; Liu, J.; Zhang, T. *Acc. Chem. Res.* **2013**, *46*, 1740−1748.
(17) Qiao, B.; Wang, A.; Yang, X.; Allard, L. F.; Jiang, Z.; Cui, Y.; Liu, J.; Li, J.; Zhang, T. *Nat. Chem.* **2011**, *3*, 634−641.
(18) Lin, J.; Wang, A.; Qiao, B.; Liu, X.; Yang, X.; Wang, X.; Liang, J.; Li, J.; Liu, J.; Zhang, T. *J. Am. Chem. Soc.* **2013**, *135*, 15314−15317.
(19) Thomas, J. M.; Raja, R. *Acc. Chem. Res.* **2008**, *41*, 708−720.
(20) Thomas, J. M.; Raja, R.; Lewis, D. W. *Angew. Chem., Int. Ed.* **2005**, *44*, 6456−6482.
(21) Wang, F.; Li, C.; Sun, L.-D.; Xu, C.-H.; Wang, J.; Yu, J. C.; Yan, C.-H. *Angew. Chem., Int. Ed.* **2012**, *51*, 4872−4876.
(22) Wang, L.; Yamauchi, Y. *J. Am. Chem. Soc.* **2010**, *132*, 13636−13638.
(23) Ding, S.-Y.; Gao, J.; Wang, Q.; Zhang, Y.; Song, W.-G.; Su, C.-Y.; Wang, W. *J. Am. Chem. Soc.* **2011**, *133*, 19816−19822.
(24) Perego, C.; Millini, R. *Chem. Soc. Rev.* **2013**, *42*, 3956−3976.
(25) Wang, C.; Wang, J.-L.; Lin, W. *J. Am. Chem. Soc.* **2012**, *134*, 19895−19908.
(26) McKittrick, M. W.; Jones, C. W. *J. Am. Chem. Soc.* **2004**, *126*, 3052−3053.
(27) Tanabe, K. K.; Siladke, N. A.; Broderick, E. M.; Kobayashi, T.; Goldston, J. F.; Weston, M. H.; Farha, O. K.; Hupp, J. T.; Pruski, M.; Mader, E. A.; Johnson, M. J. A.; Nguyen, S. B. T. *Chem. Sci.* **2013**, *4*, 2483−2489.
(28) Hackett, S. F. J.; Brydson, R. M.; Gass, M. H.; Harvey, I.; Newman, A. D.; Wilson, K.; Lee, A. F. *Angew. Chem., Int. Ed.* **2007**, *46*, 8593−8596.
(29) Canivet, J.; Aguado, S.; Schuurman, Y.; Farrusseng, D. *J. Am. Chem. Soc.* **2013**, *135*, 4195−4198.
(30) Genna, D. T.; Wong-Foy, A. G.; Matzger, A. J.; Sanford, M. S. *J. Am. Chem. Soc.* **2013**, *135*, 10586−10589.
(31) Park, T.-H.; Hickman, A. J.; Koh, K.; Martin, S.; Wong-Foy, A. G.; Sanford, M. S.; Matzger, A. J. *J. Am. Chem. Soc.* **2011**, *133*, 20138−20141.
(32) He, J.; Zha, M.; Cui, J.; Zeller, M.; Hunter, A. D.; Yiu, S.-M.; Lee, S.-T.; Xu, Z. *J. Am. Chem. Soc.* **2013**, *135*, 7807−7810.
(33) Li, H.; Zhu, Z.-H.; Zhang, F.; Xie, S.-H.; Li, H.-X.; Li, P.; Zhou, X.-G. *ACS Catal.* **2011**, *1*, 1604−1612.
(34) Mehendale, N. C.; Sietsma, J. R. A.; de, J. K. P.; van, W. C. A.; Gebbink, R. J. M. K.; van, K. G. *Adv. Synth. Catal.* **2007**, *349*, 2619−2630.
(35) Trilla, M.; Borja, G.; Pleixats, R.; Man, M. W. C.; Bied, C.; Moreau, J. J. E. *Adv. Synth. Catal.* **2008**, *350*, 2566−2574.
(36) Trilla, M.; Pleixats, R.; Man, M. W. C.; Bied, C.; Moreau, J. J. E. *Adv. Synth. Catal.* **2008**, *350*, 577−590.
(37) Li, L.; Shi, J.-L.; Yan, J.-N. *Chem. Commun.* **2004**, 1990−1991.
(38) Mehnert, C. P. *Chem. Commun.* **1997**, 2215−2216.
(39) Elhamifar, D.; Karimi, B.; Rastegar, J.; Banakar, M. H. *ChemCatChem* **2013**, *5*, 2418−2424.
(40) Mehnert, C. P.; Weaver, D. W.; Ying, J. Y. *J. Am. Chem. Soc.* **1998**, *120*, 12289−12296.
(41) Karimi, B.; Elhamifar, D.; Clark, J. H.; Hunt, A. J. *Org. Biomol. Chem.* **2011**, *9*, 7420−7426.
(42) Ping, E.; Venkatasubbaiah, K.; Fuller, T.; Jones, C. *Top. Catal.* **2010**, *53*, 1048−1054.
(43) Dutta, P.; Sarkar, A. *Adv. Synth. Catal.* **2011**, *353*, 2814−2822.
(44) Huang, Y.; Lin, Z.; Cao, R. *Chem. - Eur. J.* **2011**, *17*, 12706−12712.
(45) Budarin, V. L.; Clark, J. H.; Luque, R.; Macquarrie, D. J.; White, R. J. *Green Chem.* **2008**, *10*, 382−387.
(46) Xu, X.; Li, Y.; Gong, Y.; Zhang, P.; Li, H.; Wang, Y. *J. Am. Chem. Soc.* **2012**, *134*, 16987−16990.

DOI: 10.1021/acscatal.5b00569
ACS Catal. 2015, 5, 3752−3759

(47) Chen, X.; Engle, K. M.; Wang, D.-H.; Yu, J.-Q. *Angew. Chem., Int. Ed.* **2009**, *48*, 5094−5115.
(48) Zhang, H.; Shi, R.; Gan, P.; Liu, C.; Ding, A.; Wang, Q.; Lei, A. *Angew. Chem., Int. Ed.* **2012**, *51*, 5204−5207.
(49) Zhang, H.; Liu, D.; Chen, C.; Liu, C.; Lei, A. *Chem. - Eur. J.* **2011**, *17*, 9581−9585.
(50) Liu, C.; Zhang, H.; Shi, W.; Lei, A. *Chem. Rev.* **2011**, *111*, 1780−1824.
(51) Wang, H.; Wang, L.; Shang, J.; Li, X.; Wang, H.; Gui, J.; Lei, A. *Chem. Commun.* **2012**, *48*, 76−78.
(52) Zhao, Y.; Jin, L.; Li, P.; Lei, A. *J. Am. Chem. Soc.* **2008**, *130*, 9429−9433.
(53) Zhao, Y.; Wang, H.; Hou, X.; Hu, Y.; Lei, A.; Zhang, H.; Zhu, L. *J. Am. Chem. Soc.* **2006**, *128*, 15048−15049.
(54) Meng, L.; Liu, C.; Zhang, W.; Zhou, C.; Lei, A. *Chem. Commun.* **2014**, *50*, 1110−1112.
(55) Meng, L.; Wu, K.; Liu, C.; Lei, A. *Chem. Commun.* **2013**, *49*, 5853−5855.
(56) Kubota, A.; Emmert, M. H.; Sanford, M. S. *Org. Lett.* **2012**, *14*, 1760−1763.
(57) Vora, H. U.; Silvestri, A. P.; Engelin, C. J.; Yu, J.-Q. *Angew. Chem., Int. Ed.* **2014**, *53*, 2683−2686.
(58) Engle, K. M.; Wang, D.-H.; Yu, J.-Q. *J. Am. Chem. Soc.* **2010**, *132*, 14137−14151.
(59) Emmert, M. H.; Cook, A. K.; Xie, Y. J.; Sanford, M. S. *Angew. Chem., Int. Ed.* **2011**, *50*, 9409−9412.
(60) Zhang, Y.-H.; Shi, B.-F.; Yu, J.-Q. *J. Am. Chem. Soc.* **2009**, *131*, 5072−5074.
(61) Ye, M.; Gao, G.-L.; Yu, J.-Q. *J. Am. Chem. Soc.* **2011**, *133*, 6964−6967.
(62) Asefa, T.; MacLachlan, M. J.; Coombs, N.; Ozin, G. A. *Nature* **1999**, *402*, 867−871.
(63) Grüning, W. R.; Siddiqi, G.; Safonova, O. V.; Copéret, C. *Adv. Synth. Catal.* **2014**, *356*, 673−679.
(64) Sun, L.; Mai, W.; Dang, S.; Qiu, Y.; Deng, W.; Shi, L.; Yan, W.; Zhang, H. *J. Mater. Chem.* **2012**, *22*, 5121−5127.
(65) Takeda, H.; Ohashi, M.; Tani, T.; Ishitani, O.; Inagaki, S. *Inorg. Chem.* **2010**, *49*, 4554−4559.
(66) Waki, M.; Maegawa, Y.; Hara, K.; Goto, Y.; Shirai, S.; Yamada, Y.; Mizoshita, N.; Tani, T.; Chun, W.-J.; Muratsugu, S.; Tada, M.; Fukuoka, A.; Inagaki, S. *J. Am. Chem. Soc.* **2014**, *136*, 4003−4011.
(67) Wu, F.; Feng, Y.; Jones, C. W. *ACS Catal.* **2014**, *4*, 1365−1375.
(68) Diao, T.; Pun, D.; Stahl, S. S. *J. Am. Chem. Soc.* **2013**, *135*, 8205−8212.
(69) Pun, D.; Diao, T.; Stahl, S. S. *J. Am. Chem. Soc.* **2013**, *135*, 8213−8221.
(70) Izawa, Y.; Pun, D.; Stahl, S. S. *Science* **2011**, *333*, 209−213.
(71) Li, W. B.; Murakami, Y.; Orihara, M.; Tanaka, S.; Kanaoka, K.; Murai, K.; Moriga, T.; Kanezaki, E.; Nakabayashi, I. *Phys. Scr.* **2005**, *2005*, 749.
(72) Waser, J.; Levy, H. A.; Peterson, S. W. *Acta Crystallogr.* **1953**, *6*, 661−663.
(73) Kirik, S. D.; Mulagaleev, R. F.; Blokhin, A. I. *Acta Crystallogr., Sect. C: Cryst. Struct. Commun.* **2004**, *60*, m449−m450.
(74) Jia, C.; Lu, W.; Kitamura, T.; Fujiwara, Y. *Org. Lett.* **1999**, *1*, 2097−2100.

DOI: 10.1021/acscatal.5b00569
ACS Catal. 2015, 5, 3752−3759